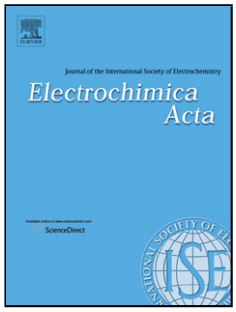

Title: Optimization of performance and stability of quantum dot sensitized solar cells by manipulating the electrical properties of different metal sulfide counter electrodes

Authors: Arumukham Manjceevan, Jayasundera Bandara

PII: S0013-4686(17)30559-5
DOI: http://dx.doi.org/doi:10.1016/j.electacta.2017.03.089
Reference: EA 29123

To appear in: *Electrochimica Acta*

Received date: 24-11-2016
Revised date: 1-3-2017
Accepted date: 12-3-2017

Please cite this article as: Arumukham Manjceevan, Jayasundera Bandara, Optimization of performance and stability of quantum dot sensitized solar cells by manipulating the electrical properties of different metal sulfide counter electrodes, Electrochimica Actahttp://dx.doi.org/10.1016/j.electacta.2017.03.089

Optimization of performance and stability of quantum dot sensitized solar cells by manipulating the electrical properties of different metal sulfide counter electrodes

Arumukham Manjceevan, Jayasundera Bandara*

National Institute of Fundamental Studies, Hantana Road, Kandy, CP 20000, Sri Lanka.
E-mail:bandaraj@ifs.ac.lk, jayasundera@yahoo.com

Highlights

- Solar cell performances and stability of different counter electrodes were tested.
- Cell performance highly depended on electrical properties of counter electrodes.
- Charge transfer resistance and attachment of CE material is an important factor.
- The Cu_2S electrodeposited on brass express better counter electrode properties.

Abstract

Fabrication of low cost and high catalytic active counter electrode (CE)for quantum dot sensitized solar cells is one of the dynamic ways to enhance the performance of quantum dot solar cell. In this investigation, different CE materials such as copper sulfide (Cu_2S), cobalt sulfide (CoS) and nickel sulfide (NiS) were deposited on fluorine doped tinoxide (FTO) glass and brass plate by single step electrophoretic deposition technique and solar cell performance and stability of three different CEs were tested. Electrochemical deposition parameters were optimized for the optimization of CEs performance. Electrical properties of Cu_2S, CoS and NiS CEs were investigated by electrochemical impedance spectroscopy and electrical properties were compared with the observed solar cell performances and stability.Of the tested CEs materials, enhanced solar cell performance was observed with Cu_2S CE than the CoS or NiS CEs while brass substrae was found to be a better substrate than FTO for these CE materials. The optimized Cu_2S/brass plate CE showed current density of (Jsc) 17.9 $mA.cm^{-2}$, open circuit voltage of (Voc) 494.5 mV, fill factor of (FF) 59.0% and efficiency of 5.2% with the solar cell fabricated with PbS/CdS q-dot anode. While Cu_2S/FTO glass plate CE showed Jsc of 16.1 $mA.cm^{-2}$, Voc of 489.4 mV, FF of 52.9% and efficiency of 4.2 % of with the same q-dot anode.A higher electrocatalytic activity together with the lower charge

transfer resistance (Rct) and good inter-connected Cu_2S particles on brass electrodes were found to be the major CE properties that decides the performance of CE.

Keywords: PbS/CdS, quantum dot, counter electrodes, solar cell, Brass/Cu_2S.

1. Introduction

Quantum dot sensitized solar cells (QDSCs) are promising next generation solar cells due to their characteristic features like tunable band gaps, multiple electron/hole generation and simple fabrication procedures[1, 2]. Quantum dot (Q-dot) sensitized solar cells typically have similar configuration as in the dye sensitized solar cells (DSSCs) in which q-dots act as sensitizers in QDSCs [3]. Despite QDSCs have similar configuration to that of DSSCs, the highest reported efficiencies for CdSeTe[4], CdS/CdSe[5] and PbS/CdS[6] QDSCs are 8.0, 7.1 and 5.7%respectively. Hence, the power conversion efficiencies of QDSCs are still far below than the power conversion efficiencies of DSSC with porphyrin sensitizer 13% [7] as well as perovskite materials 15% [8].

The inferiorsolar cell efficiencies of QDSCs could be mainly attributed to; (a) rapid electron loss due to recombination of excited electron in TiO_2 and/or in q-dots with electrolyte[4, 9, 10] and (b) energy loss in between counter electrode and electrolyte interface[11, 12]. Therefore, in order to enhance the performance of QDSCs, research has been focused mainly on minimizing of charge recombination in TiO_2 interface as well as minimizing energy loss between the counter electrode and the electrolyte interface. Hence, the optimization of CE is an imperative to improve the performance of QDSSCs. Counter electrodes such as CoS/FTO[1, 13], NiS/FTO[14], Cu_2Se/FTO[15] and Ni_2Se/FTO[15], Pt/FTO[16-18], Cu_2S/FTO[1, 16,

17, 19-21], PbS/FTO[22], $Cu_2ZnSnSe_4$[23] and NiS[1, 14] have been investigated as possible alternative counter electrodes to optimize the performance of QDSCs.Previous study revealed that the energy loss between the counter electrode-electrolyte interface is one of the major reasons that contributes to poor fill factor and low efficiency of QDSSCs[11, 12]. Hence, good catalytic activity of CE for the reduction of oxidized redox species of the electrolyte is an important parameter for better performance QDSSCs solar cell.

In the case of DSSCs, the platinum CE exhibits unchallenged catalytic activity with I_3^-/I^- redox couple electrolyte. However, Pt shows poor CE properties with polysulfide electrolytes due to strong chemisorption of electrolyte on Pt CE [3, 24] resulting in poor solar cell efficiency in q-dot sensitized solar cell. On the other hand, polysulfide electrolyte with metal sulfides CE exhibits more desired properties than I_3^-/I^- redox couple due to photocorrosion of metal sulfides by I_3^-/I^- species causing in rapid deterioration of solar cell performance[12].It is known that the CE properties such as resistance to photocorrosion, reduced charge transfer resistance and high catalytic activity are the desired properties of a CE of a QDSC[12, 14, 19, 25]. Owing to their high conductivity, good catalytic activity and more importantly due to less charge transfer resistance properties, CoS and Cu_2S materials on FTO are considered to be the good CEs for QDSCs [11, 12].However, the stability is the major concern of CoS and Cu_2S counter electrodes due to corrosion of these materials and hence stability of CE is one of the major bottlenecksin Q-dot solar cell research [12].Finding of stable alternative CE materials and substrates for q-dot solar cell is imperative for further improvement of the q-dot solar cell performance as well as for long term stability of q-dot solar cells.The main objective of this report is to investigate different CE materials and substrates as possible CEs for q-dot solar cells. In this

investigation, different metal sulphides such as CoS, NiS and Cu_2S were deposited on different substrates such as FTO and brass. The CE properties of CoS, NiS and Cu_2S on FTO and brass substrates were investigated against the PbS/CdS sensitized photoanode on FTO. The performances and stability of PbS/CdS QDSCs with different counter electrodes were correlated to surface, electrocatalytic properties as well as electronic properties of such counter electrodes for the first time.

2. Experimental Section

2.1 Preparation of Cu_2S, CoS and NiS counter electrodes

FTO glass (Soloronix: sheet resistance 15 $\Omega.cm^{-2}$: thickness 2mm) and brass plate (0.65 $\Omega.cm^{-2}$: thickness 1.24 mm) were ultrasonically cleaned in the detergent and washed in cold deionized water, hot deionized water and ethanol sequentially and finally dried off by using hot plate. Different sulfide materials on CE electrodes were electrodeposited either on top of FTO or brass conducting surfaces by single step electrodeposition method with the three electrode system using Pt, Ag/AgCl and FTO glass (or brass plate) as counter, reference and working electrodes respectively.For the deposition of Cu_2S, an electrolyte consisting of 40 ml of 0.05 M $CuSO_4.5H_2O_{(aq)}$ and 0.15 M $Na_2S_2O_3.5H_2O_{(aq)}$ in the 150 ml beaker was employed and electrodeposition of was performedat -1.1V for four minutes. After deposition of Cu_2S, the electrode was dried off by using air blower, washed by deionized water and again dried off consecutively. Finally, the Cu_2S deposited CE was treated with 0.1M $Na_2S_{(aq)}$ and 0.1M S for one minute and rinsed with deionized water and ethanol. In a similar manner, for the preparation of CoS CEs on either on FTO or brass, CoSwas electrodeposited by using electrolytes containing of 0.05 M $CoSO_4.5H_2O_{(aq)}$ and 0.15 M $Na_2S_2O_3.5H_2O_{(aq)}$at -1.1 V for four minutes. For the electrodepositon of NiS either

on FTO or brass, 0.05 M $NiSO_4$, 0.15 M $Na_2S_2O_3.5H_2O_{(aq)}$electrolyte was employed at the electrodepositon was carried out at -0.85 V for four minutes. The CEs fabricated with Cu_2S, CoS and NiS on FTO glass and brass plate were denote as A, B, C, D, E and F respectively while platinum counter electrode is denote as G.

2.2 Fabrication of solar cell device

For the fabrication of solar cell, as a first step, a compact TiO_2 layer was deposited on FTO. To fabricate a compact TiO_2 layer on bare FTO, 20 µl of a mixture containing of Titaniumisopropoxide (0.177 ml, 97%, Fluka), diethanolamine (0.1 ml, 99%, Fluka) in butan-1-ol (1.822 ml, 99%, AnalaR) were spin coated at 5000 rpm and dried at 130^{o}C for five minutes. The coating and drying process were repeated for three times and finally sintered at 500^{o}C for 45 minutes. On top of the compact TiO_2 layer, a 15 µm TiO_2 mesoporous layer was fabricated by doctor blade method using DyesolTiO_2 paste (DSL 18-NRT, 20 nm average particle size) and TiO_2 paste prepared by modified Pichini methods. The modified Pichini based sol-gel preparation methods 1 (TiO_2Pichini1) and 2 (TiO_2Pichini2) have been detailed in our previous publication[6]. In the fabrication of TiO_2 mesoporous layer following steps were taken; (a) Dysol paste was doctor bladed with two scotch tape thickness and sintered at 500^{0}C for 30 minutes, (b) on top of the Dyesol TiO_2 layer, a layer of TiO_2Pichini1 was doctor bladed with two scotch tape thickness[26] and sintered at 450^{0}C for 30 minutes with 3^{0}C/minutes ramping of temperature, (c) finally, TiO_2Pichini2 was doctor bladed with two scotch tape thickness and sintered.

The SILAR method (successive ion layer adsorption and reaction) was employed to deposit Q-dots on mesoporous TiO_2photoanode. As reported in our earlier work[6], PbS, CdS, ZnS were coated on TiO_2photoanode by SILAR method. In brief, the bare TiO_2photoanode was immersed in a solution containing 3-

mercaptoproponic acid (0.015M) and 0.02M $Na_2S_{(aq)}$ solution for 1.5 minutes followed by immersing into the 0.02M $Pb(Ac)_{2(aq)}$ solution for 1.5 minutes. Extra $Pb(Ac)_2$ was removed by washing with methanol. To convert adsorbed Pb into PbS, Pb adsorbed TiO_2photoanodefilm was again immersed into a solution containing 0.015M 3-mercaptoproponic acid and 0.02M $Na_2S_{(aq)}$. The whole process is labeled as one cycle of PbS deposition. Likewise, for CdS and ZnS deposition, the above process was repeated using either 0.05M $Cd(Ac)_{2(aq)}$or 0.05M $Zn(Ac)_{2(aq)}$ as cationic species and mercaptoproponic acid mixed 0.05M $Na_2S_{(aq)}$ as anionic solutions respectively. In a typical photoanode fabrication, one cycle of PbSwas deposited first on TiO_2 and three cycles of CdSwere deposited on the PbS layer by SILAR deposition method and finally deposition was completed with two cycles of ZnS deposition. Finally, the q-dot sensitized photoanodeand the counter electrode were sandwiched by placing a parafilm spacer in between photoanode and the CE. A liquid electrolytewas prepared with 2M Na_2S, 2M S and 0.2M KCl in water: methanol mixture of 3: 7 ratio and the assembled solar cell was filled with 20 µl of electrolyte.

2.3 Characterization

Fabricated CE materials were characterized by using x-ray diffraction (XRD) measurements, VU-visible spectroscopic measurements, Scanning Electron Microscopy (SEM) analysis, cyclic voltammetry analysis, electrochemical impedance analysis (EIS) and Tafel polarization measurements. The XRD measurements were performed by using powder diffraction (Siemens D5000 X-ray diffractometer with Cu Kα radiation operating at 40 KV, scanning from $2\theta = 20$ to 80º). Morphology of the counter electrodes were observed by Carl Zeiss EVO LS 15 scanning electron microscope.Photovoltaic performance (current-voltage curve) were measured using

Keithley 2400 source meter under illumination using a solar simulator at AM1.5G (Newport AAA solar simulator at 100 mW/cm^2). The intensity of solar simulator was calibrated with standard Si-reference cell. Active area of photovoltaic cell was 0.159 cm^2. External quantum efficiency (EQE) was measured as the function of wavelength from 300 nm to 1100 nm using Bentham PVE300 unit with a TMc300 monochromator based IPCE with the Xenon arc lamp. The EIS measurements were performed under dark conditions by using Zahner Zannium universal electrochemical work station equipped with a frequency response analyzer (Thalas) in the frequency range from 0.1 Hz to 1MHz and 10 mV amplitude ac signal[27]. For EIS measurements, two symmetric counter electrodes with an active area of 0.6 X 0.5 cm^2 were sandwiched in face to face manner and electrolyte was applied in between them.

3. Results and discussion

In this study Cu_2S, CoS and NiSCEs on FTO or brass substrate were fabricated by single bath electrophoretic deposition involving respective cationic and anionic sources of corresponding metals (M – Cu, Co and Ni) and thiosulfate ion solutions. The reactions leading to formation of metal sulfide ($MS_{(s)}$ – Cu_2S, CoS and NiS) on the FTO or brass substrate are given in reactions (1) to (3).

$$S_2O_3^{2-}{}_{(aq)} + H^+{}_{(aq)} \rightarrow S_{(s)} + H_2SO_3{}_{(aq)} + 2H_2O_{(l)} \quad (1)$$

$$S_{(s)} + 2H^+_{(aq)} + 2e \rightarrow H_2S_{(aq)} \quad (2)$$

$$M^{2+}_{(aq)} + S^{2-}_{(aq)} \rightarrow MS_{(S)} \quad (3)$$

The performance of CEs were tested with q-dot sensitized photoanode. The photoanode was fabricated with q-dot PbS on mesoporous TiO_2 particles on FTO[6]. PbS was deposited on TiO_2 by using MPA linker molecule and the MPA covalently attach the PbS to the TiO_2 surface. The molecular structure of MPA contains a thiol (–SH) group on one end and a

carboxylic acid group (–COOH) on the other end. The carboxylic acid is attracted to the surface of the TiO_2while the thiol group of MPA is attracted to the PbS forming disulfide bonds. The average size of MPA assited growth q-dot PbS particles is ~ 5 nm[28].

Photovoltaic performances of different types of counter electrodes

To compare the solar cell performance and the catalytic activities of different CEs, the solar cell performances of PbS/CdS q-dot on mesoporous TiO_2 film were compared with different CEs. The J-V curves of PbS/CdS QDSC with Cu_2S/FTO,CoS/FTO, NiS/FTO CEs and Cu_2S/brass,CoS/brass, NiS/brass CEs are shown in Figure 1a and 1b respectively. For the comparison purpose, solar cell performance of Pt CE is also included in Figure 1a and 1b. The corresponding photovoltaic parameters extracted from the *J–V* curves are given in Table 1.

As given in Table 1, PbS/CdS q-dot photoanode with Cu_2S electrodeposited on top of brass plates gives current density of (Jsc) 17.9 $mA.cm^{-2}$, voltage of (Voc) 494.5 mV, fill factor of (FF) 59.0% and efficiency (η) of 5.2 %, while Cu_2S electrodeposited on top of FTO glass plates shows Jsc of 16.1 $mA.cm^2$, Voc of 489.4 mV, FF of 52.9% and η of 4.2%. The solar cell performance parameters indicate a slightly improvement in Voc for Cu_2S on brass than that of on FTO counter electrodes. However, significant improvements in Jsc and FF could be observed with Cu_2S/brass CE than that of Cu_2S/FTO glass CE. As given in Table 1, it can be noted the same trend of performances with CoS/brass CE and NiS/brass CE. Enhanced Voc, Jsc and FF were noted with CoS/brass andNiS/brass CEs than that of CoS/FTO andNiS/FTO CEs. However, among the various CEs tested, the highest Jsc is noted with both CoS/FTO and CoS/brass CEs despite CoS exhibits inferior Voc, FF and η than that of Cu_2S. The enhanced Jsc with CoS CE material could be due to several factors such as

enhanced surface roughness and better charge collection which need to be further investigated.Importantly, it was noted that the solar cell performance of PbS/CdS with Pt CE is far inferior to that of metal sulfide/brass or metal sulfide/FTO CE which is due to decrease of catalytic activity as a result of poisoning of Pt by the polysulfide electrolyte[19].

The variation of Jscs and spectral response for PbS/CdS q-dot solar cells with Cu_2S, CoS and NiS on FTO glass and brass substrate is further confirmed by the IPCE measurement as shown in Figure 1c and 1d. The IPCE of PbS/CdS q-dot solar cels with Cu_2S/FTO, CoS/FTO, NiS/FTO CEs are shown in Figure 1c while the same with Cu_2S/brass, CoS/brass, NiS/brass CEs are shown in Figure 1d. It is clear that the different CEs fabricated with Cu_2S, CoS and NiS on both brass and FTO substrates have similar spectral response with photoanodePbS/CdS where IPCE maximum around 550 nm and extend up to near IR regions. However, the generation of high photocurrent in the brass substrate based Cu_2S, CoS and NiS CEs than the FTO substrate based Cu_2S, CoS and NiS CEs are clearly evident from IPCE justifying the J-V characterization. Additionally, CoS exhibits better IPCE characteristics than that of Cu_2S justifying the observed higher Jsc with CoS CE.

Both J-V and IPCE measurement results indicate that the brass as substrate for the CE is better than that of FTO for q-dot sensitized solar cells. It is known that the superb electro-catalytic activity and good inter-connected CE materials are the major required properties of CE material and CEs resulting in improved charge transfer process and hence superior solar cell performance[3, 29]. Hence in the following sections, the electrochemical properties as well as optical and structural properties of different CEs were investigated to justify the superior performance of CE fabricated with brass and Cu_2S.

Structural and morphological characterization of counter electrodes

Surface SEM images of Cu_2S/FTO, Cu_2S/brass, CoS/FTO, CoS/brass, NiS/FTO and NiS/brass are given in Figure 2a, b, c, d, e and f respectively and the corresponding cross sectional images of the same are given in supporting information (SI) of Figure S1, a, b, c, d, e and f respectively. As shown in Figure 2a and b, distinct differences in Cu_2S on brass and Cu_2S on FTO are clearly observable in which Cu_2S/FTO composed of tightly packed arrangement while Cu_2S/brass composed of ~80 nm Cu_2S nanoparticles packed in a highly porous manner (with some aggregates of Cu_2S). Similarly, differences in SEM images of CoS and NiS on brass and CoS and NiS on FTO are noted where in both CoS/FTO and NiS/FTO, large clumps of CoS (or NiS) are noticed while in CoS/brass and NiS/brass, smaller clumps of CoS (or NiS) are clearly visible, yielding higher surface area and roughness when brass is used as substrate. In general, Cu_2S particles on brass plate have rough surface than CoS or NiS CEs. The high roughness of Cu_2S particles on brass CE results in greater surface area which will undoubtedly facilitate electro-catalytic activity between counter electrode and electrolyte by transferring the electron on the back contact to the reaction site rapidly[19]. Hence, for PbS/CdS Q-dot solar cells, enhanced solar cell performance can be expected with Cu_2S/brass CE compared to CoS or NiS CEs.

The crystal phases of CE materials were done by XRD analysis while the optical characterizations were done byUV-Visible absorbance measurements and the results are shown in Figure 3 and Figure S2respectively. As shown in Figure 3,XRD analysis of Cu_2S, CoS and NiS on FTO confirm the presence of hexagonal Cu_2S and cubic structures of Co_9S_8 and NiS_2 which are non-stoichiometric sulfides[30-32]. However, weak and broad XRD peaks indicate the lack of crystallinity at low

temperature fabrications. Copper sulfide, cobalt sulfide and nickel sulfides were in Cu_2S, $Co_9S_8$and NiS_2form. Cu_2S shows the XRD peak positions of hexagonal structure (a=b= 3.96 and c=6.78, JCPDS No. 46-1195) and CoS, NiS peak positions were also clearly matched with cubic structure of Co_9S_8 (a=b=c= 9.907, JCPDS No. 03-0631) and NiS_2 (a=b=c= 5.6196,JCPDS No. 80-0375) respectively. Similarly, XRD analysis of Cu_2S, CoS and NiS on brass showed hexagonal Cu_2S and cubic Co_9S_8 and NiS_2.Based on above XRD interpretations,the formation of Cu_2S,CoS and NiS can be confirmed. Diffuse reflectance spectra of Cu_2S, CoS and NiS on FTO and brass are shown in Figure S2 of SI and the optical measurements indicate broad absorption characteristics of CoS than that of Cu_2S or NiS, while Cu_2S and NiS exhibit higher reflection than that of CoS.

Electro-catalytic properties of different counter electrodes

In order to study the electrochemical behavior of CEs, cyclic voltammetry analysis of different CEs were performed. The CV measurements were performed with an electrolyte consisting of 0.1 M Na_2S, 0.1 M S in deionized water by using Ag/AgCl sat KCl, Ptand metal sulfides/FTO glass or metal sulfides/brass plate electrodes as reference, counter and working electrodes respectively.In CV analysis, the catalytic behaviors of CEs were assessed by current densities at cathodic and anodic peak positions. It is known thatthe cathodic peak to anodic peak separation inversely proportion to electrochemical rate constant of redox reaction[2]. The CVs of Cu_2S, CoS, NiS on FTO and Cu_2S, CoS,NiS on brass are given in Figure 4a and b respectively and the peak to peak splitting (Epp) derived from the CVs of Figure 4a,b are given in Table 2. Additionally, CV of Pt CE is also given in Figure 4b for reference. As given in the Table 2, among the CEs tested, Epp of metal sulfide/brass is always lower than that of the

metal sulfide/FTO. The lower Epp of brass substrate indicates a higher electrocatalytic activity of brass substrate than that of FTO substrate and hence brass substrate is moresuitable for CE for q-dot sensitized solar cells. On the other hand, the Epp of the CoS/brass CE has the lowest value among CuS, CoS, and NiS on brass despite cathodic current density at peak position exist in the order of Cu_2S>CoS>NiS, among different metal sulfide/brass CEs. A lower Epp of CoS implies that a higher electrochemical rate constant or the catalytic activity of CoS/brass CE than Cu_2S or NiSCEs.Higher catalytic activity or the electrochemical rate constant of CE is directly resulting in enhanced Jsc which is evidenced by the observed higher Jsc of the PbS/CdS electrode when CoS/brass was used as the CE (Table 1).On the other hand, observed higher cathodic current densities with the CE of Cu_2S and CoS at peak positions of respective CV analysis, indicative of good catalytic activity of Cu_2S and CoS among other sulfide counter electrodes considered for the analysis.

Interestingly, as shown in Figure 4b, curve G and Table 2, the observed small Epp value of the Pt counter electrode is indicative of higher catalytic activity of the Pt CE, which is also represented by the observed fairly good photocurrent when Pt was used as CE with the PbS/CdS q-dot sensitized solar cell. However, a lower cathodic current density was observed with Pt CEs in CV analysis which could be due to chemisorption of sulfur species of electrolyte resulting in poisoning of Pt counter electrode and in turn, this will lead to poor fill factor and efficiency as well and hence Pt is found to be a inferior CE for q-dot solar cells with polysulphide electrolyte[2, 19]. These results indicate that Pt CE is not a suitable CE for Q-dot solar cells with polysulfide electrolyte.

Additionally, we also performed multi-cycle CV scan to analyze the stability of the different metal sulfide/CEs. Multi-cycle CV scans of Cu_2S/FTO and Cu_2S/brass

substrates are shown in Figure 5a. In Figure 5b, multi-cycle CV scans of CoS/FTO and CoS/brass substrates are shown and while in Figure 5c, multi-cycle CV scans of NiS/FTO and NiS/brass substrates are shown.As shown in the Figure 5a,b and c, on brass substrate, Cu_2S, CoS and NiS exhibit fairly steady current densities than that of FTO substrate under similar conditions. Fairly steady current densities on brass substrate indicate that metal sulfides deposited on brass substrate express more stability than on the FTO glass plates. Moreover, according to the Figure5a and 5b,cathodic peaks of Cu_2S/brass (curve D in Figure 5a) varies slightly with number of cycle of CV while cathodic peaks of CoS/brass (curve E in Figure 5b) remain in the same position indicating that the CoS/brass CE exhibits more stability than the Cu_2S/brass counter electrode in the presence of polysulfide electrolyte.

To further substantiate the stability of Cu_2S as CE material, we performed the stability test of PbS/CdS q-dot solar cell with Cu_2S/FTO and Cu_2S/brass CEs. In Figure 6a, the variation of Jsc of PbS/CdS solar cell with the time is shown for both Cu_2S/FTO and Cu_2S/brass CEs. While Figure 6b, c and d exhibit the temporal variation of Voc, FF and η respectively for Cu_2S/FTO and Cu_2S/brass CEs with PbS/CdS q-dot solar cells. As shown in the Figure 6a, b, c and d, it is clearly evident that Voc and FF remain fairly stable with both Cu_2S/brass and Cu_2S/FTO substrates. However, the Jsc is found to be decreasing in faster rate with Cu_2S/FTO CE while with Cu_2S/brass CE,the observed Jsc is was found to be stabilized after initial drop. (Initially due to corrosion of CE by polysulfide) Consequently, PbS/CdS Q-dot solar cells fabricated with Cu_2S/brass CE exhibits enhanced stability compared with solar cells fabricated with Cu_2S/FTO CE.

To ensure the results obtained from cyclic voltammetry analysis, we performed the EIS analysis of different CEs with symmetric dummy cell arrangement [19, 33].

Figure 7 shows the Nyquist impedance plots of different metal sulfides on brass and FTO substrates. The EIS analyses were performed by fitting the parameters with equivalent circuit model shown in the inset in Figure 7. The Rs (series resistance), Rct (charge transfer resistance) and Z_N(diffusion impedance of electrolyte) were extracted and the derived data from impedance spectra for Rs and Rct are summarized in Table 3. The fitting errors were calculated by using Z-view software [34] and chi-square goodness-of-fit (χ^2) and sum of squares (ss) are shown in Table 3 where χ^2 is proportional to the error between the fittings and the measurements, and ss reflects the total error percentage difference. As shown in Table 3, $\chi^2$and ss values indicate farily good fittings of experimental EIS measurements. As in working conditions of the solar cells, various resistance and capacitance exist in materials or at the interface between the materials play significant role on the flow of charges[3]. In symmetric dummy cell arrangement of the EIS analysis, the intercept of arc at high frequency regiongives Rs and arc of first semicircle provides the information about Rct and the arc of second semicircle provides Z_N.The measurement of charge transfer resistance at CEs provides an indication of the catalytic activity of CEs. A lower Rctvalue of counter electrode suggests a faster redox reaction of counter electrodes/electrolyte interface resulting in rapid regeneration of oxidized electrolyte species and hence enhanced solar cell efficiency[3].

The observed Rct values of Cu_2S, CoS and NiS on both brass and FTO substrates varied in the range 1-15Ω cm^2 while Rct values on brass is always lower than that of FTO. The lower Rct values of brass could be due to the effect the electronic transition properties between electrolytes and counter electrodes of substrate materials. It is interesting to note of having lower Rct values for both Cu_2S and CoS on brass and FTO (for Cu_2S/brass and Cu_2S/FTO, the observed Rctvalues are 1.4 and

1.6Ω cm^2 respectively, while for CoS/brass and CoS/FTO, the observed Rct values are 3.7 and 4.8Ωcm^2respectively). These results reinforce that Cu_2S and CoS exhibit good counter electrode properties which will agree and confirm the reported higher solar cell performance of PbS/CdS q-dots solar cells with Cu_2S/brass and CoS/brass CEs in this study.On the otherhand, Pt CE exhibit enormous Rct value with polysulfide electrolyte and leads to lower fill factor and photon to current conversion efficiency due to its chemisorption and poisoning effect of sulfide species with Pt counter electrodes[3, 19]. The EIS results clearly strengthen the prediction of CV analysis presented for different CE materials.

In addition to charge transfer behavior, EIS analysis also provides morphological information of counter electrodes. The constant phase element (CPE) of EIS analysis reflect the interfacial capacitance and consider the roughness of surface effect the CPE and it depress the arc of semi-circle to an ellipse form in the Nyquist plot[15, 35]. Interfacial capacitance of CEcan be expressed by the equation as $Z_{CPE} = A(j\omega)^{-\propto}$,where ω is angular frequency and A and α are frequency independent parameters[15]. The α takes the values from 0 to 1 where α tends to approach zero with depression of semicircle while for the simple capacitor behavior, α takes the value of 1. The value of α reflects the capacitance of CPE and its variation may arise due to change in porosity of electrode surface[35]. Therefore, variations of constant phase element (CPE) and α could associate with variation of roughness and porosity of electrodes[15]. The calculated CPE values from EIS analysis of different CEs are given in Table 3. It is clear that the Cu_2S on brass and FTO exhibit higher CPE and lower values of α. In other word, Cu_2S CEs have higher roughness and porosity than theCoS and NiSCEs. SEM images of counter electrodes shown in Figure 2 reinforce the above prediction that Cu_2S counter electrodes exhibits high rough

surfaces. Hence higher roughness and porosity of CE provide higher contact areas between electrolyte and CE resulting in increase in charge transfer rates yielding enhanced solar cell performance of Cu_2S/brass and Cu_2S/FTO CEs.

As Tafel polarization measurement provides additional proofs to the catalytic behavior of counter electrodes, Tafel polarization plot of Cu_2S, CoS and NiS on both brass and FTO were investigated and shown in Figure 8a and b respectively. In Tafel curve, three different zones such as polarization zone (voltage approximately between $\leq \pm 120$ mV), diffusion zone (moderately higher voltage region)and Tafel zone (in between polarization and diffusion zones) can be identified[3]. The limiting current density J_{lim}at saturated charge transfer rate which can be obtained by read value of flat current density value of Tafel plot. Theoretically, J_{lim}value independent of over potential but it depends on other factors like adsorption, catalytic activity and diffusivity. According to equation (4) J_{lim} value proportionally correlate with diffusion coefficient.

$$D = \frac{\delta}{2nFC} J_{lim} \qquad (4)$$

Where D, δ, n, F, C referred as diffusion coefficient, spacer thickness, number of electron involved in the reduction reaction, Faraday constant and concentration of electrolyte species respectively. Therefore, J_{lim} is an important counter electrode property that describes the maximum value of transferred current density and diffusion coefficient for polysulfide redox couple[2]. Estimated diffusion coefficient values are given in Table 3. The estimated diffusion coefficients of Cu_2S and CoS on brass as well as on FTO are not significantly different (diffusion coefficient of CoS counter electrodes are marginally higher than that of Cu_2S counter electrode). Comparatively,

diffusion coefficients of NiS/FTO ($0.83x10^{-6}$ cm^2s^{-1}) and NiS/brass ($0.85\ x10^{-6}$ cm^2s^{-1})are very smaller than that of Cu_2S or CoS. These results further substantiate the superior counter electrode property of Cu_2S/brass and CoS/brass CEs. Interestingly, the exchange current density (J_0) (in Figure8) are in the order of Cu_2S>CoS>NiS and further, materials on brass get higher J_0 value than respective sulfides on FTO glass. It confirm the superior CE properties of Cu_2S and CoS on brass where higher J_{limit} and J_o values of counter electrodes conjecture with good counter electrode properties.

CONCLUSION

In conclusion, Cu_2S, CoS and NiS counter electrodes were successfully fabricated by single step electrophoretic deposition with three electrode system. The Cu_2S counter electrode has good counter electrodes properties like lower Rct, higher cathodic current density, higher exchange current density, higher surface roughness and higher porosity. The CoS also have some best characteristic features like slightly lower peak to peak splitting potential values in the cyclicvoltammetryanalysis, better stability and higher limiting current density in Tafel polarization curve as well. The stability and the efficiency of counter electrode increase by using brass substrate than FTO glass due to higher attachment of Cu_2S with brass and higher charge transfer rate between counter electrode and electrolyte. Finally, the Cu_2S electrodeposited on brass express better counter electrode properties and it produce high efficiency of PbS/CdS quantum dot sensitized solar cells.However, CoS is a promising CE material for q-dot solar cells which produces higher Jsc with PbS/CdS than Cu_2S or NiS CE material.If catalytic activity and charge transfer process can be increased, CoS would be a better CE material than Cu_2S for q-dot solar cells. On the other hand, Pt is not a suitable CE for Q-dot solar cells with polysulfide electrolyte.

References

[1] Z. Yang, C.-Y. Chen, C.-W. Liu, H.-T. Chang, Electrocatalytic sulfur electrodes for CdS/CdSe quantum dot-sensitized solar cells, Chem. Commun., 46 (2010) 5485-5487.
[2] I. Hwang, K. Yong, Counter Electrodes for Quantum-Dot-Sensitized Solar Cells, ChemElectroChem, (2015).
[3] I. Hwang, K. Yong, Counter Electrodes for Quantum-Dot-Sensitized Solar Cells, ChemElectroChem, 2 (2015) 634-653.
[4] K. Zhao, Z. Pan, I. Mora-Sero, E. Canovas, H. Wang, Y. Song, X.-Q. Gong, J. Wang, M. Bonn, J. Bisquert, Boosting Power Conversion Efficiencies of Quantum Dot Sensitized Solar Cells Beyond 8% by Recombination Control, J. Am. Chem. Soc., (2015).
[5] Y. Bai, C. Han, X. Chen, H. Yu, X. Zong, Z. Li, L. Wang, Boosting the efficiency of quantum DoT sensitized solar Cells up to 7.11% through simultaneous engineering of photocathode and photoanode, Nano Energy, (2015).
[6] A. Manjceevan, J. Bandara, Robust surface passivation of trap sites in PbS q-dots by controlling the thickness of CdS layers in PbS/CdS quantum dot solar cells, Sol. Energy Mater. Sol. Cells, 147 (2016) 157-163.
[7] S. Mathew, A. Yella, P. Gao, R. Humphry-Baker, B.F.E. Curchod, N. Ashari-Astani, I. Tavernelli, U. Rothlisberger, M.K. Nazeeruddin, M. Grätzel, Dye-sensitized solar cells with 13% efficiency achieved through the molecular engineering of porphyrin sensitizers, Nat. Chem., 6 (2014) 242-247.
[8] M. He, D. Zheng, M. Wang, C. Lin, Z. Lin, High efficiency perovskite solar cells: from complex nanostructure to planar heterojunction, Journal of Materials Chemistry A, 2 (2014) 5994-6003.
[9] I. Mora-Seró, S. Giménez, F. Fabregat-Santiago, R. Gómez, Q. Shen, T. Toyoda, J. Bisquert, Recombination in Quantum Dot Sensitized Solar Cells, Acc. Chem. Res., 42 (2009) 1848-1857.
[10] S. Rühle, S. Yahav, S. Greenwald, A. Zaban, Importance of Recombination at the TCO/Electrolyte Interface for High Efficiency Quantum Dot Sensitized Solar Cells, The Journal of Physical Chemistry C, 116 (2012) 17473-17478.
[11] H. Chen, L. Zhu, H. Liu, W. Li, ITO Porous Film-Supported Metal Sulfide Counter Electrodes for High-Performance Quantum-Dot-Sensitized Solar Cells, The Journal of Physical Chemistry C, 117 (2013) 3739-3746.
[12] Z. Yang, C.-Y. Chen, C.-W. Liu, C.-L. Li, H.-T. Chang, Quantum Dot–Sensitized Solar Cells Featuring CuS/CoS Electrodes Provide 4.1% Efficiency, Advanced Energy Materials, 1 (2011) 259-264.
[13] M. Que, W. Guo, X. Zhang, X. Li, Q. Hua, L. Dong, C. Pan, Flexible quantum dot-sensitized solar cells employing CoS nanorod arrays/graphite paper as effective counter electrodes, Journal of Materials Chemistry A, 2 (2014) 13661-13666.
[14] H.-J. Kim, S.-W. Kim, C.V.V.M. Gopi, S.-K. Kim, S.S. Rao, M.-S. Jeong, Improved performance of quantum dot-sensitized solar cells adopting a highly efficient cobalt sulfide/nickel sulfide composite thin film counter electrode, J. Power Sources, 268 (2014) 163-170.
[15] H.M. Choi, I.A. Ji, J.H. Bang, Metal Selenides as a New Class of Electrocatalysts for Quantum Dot-Sensitized Solar Cells: A Tale of Cu1. 8Se and PbSe, ACS applied materials & interfaces, 6 (2014) 2335-2343.
[16] T. Ha Thanh, D. Huynh Thanh, V. Quang Lam, The CdS/CdSe/ZnS Photoanode Cosensitized Solar Cells Basedon Pt, CuS, Cu2S, and PbS Counter Electrodes, Advances in OptoElectronics, 2014 (2014) 9.
[17] J. Xiao, X. Zeng, W. Chen, F. Xiao, S. Wang, High electrocatalytic activity of self-standing hollow NiCo 2 S 4 single crystalline nanorod arrays towards sulfide redox shuttles in quantum dot-sensitized solar cells, Chem. Commun., 49 (2013) 11734-11736.
[18] C. Justin Raj, K. Prabakar, A. Dennyson Savariraj, H.-J. Kim, Surface reinforced platinum counter electrode for quantum dots sensitized solar cells, Electrochim. Acta, 103 (2013) 231-236.

[19] K. Zhao, H. Yu, H. Zhang, X. Zhong, Electroplating Cuprous Sulfide Counter Electrode for High-Efficiency Long-Term Stability Quantum Dot Sensitized Solar Cells, The Journal of Physical Chemistry C, 118 (2014) 5683-5690.
[20] N. Balis, V. Dracopoulos, K. Bourikas, P. Lianos, Quantum dot sensitized solar cells based on an optimized combination of ZnS, CdS and CdSe with CoS and CuS counter electrodes, Electrochim. Acta, 91 (2013) 246-252.
[21] Y.-Y. Yang, Q.-X. Zhang, T.-Z. Wang, L.-F. Zhu, X.-M. Huang, Y.-D. Zhang, X. Hu, D.-M. Li, Y.-H. Luo, Q.-B. Meng, Novel tandem structure employing mesh-structured Cu< sub> 2</sub> S counter electrode for enhanced performance of quantum dot-sensitized solar cells, Electrochim. Acta, 88 (2013) 44-50.
[22] M.A. Abbas, M.A. Basit, T.J. Park, J.H. Bang, Enhanced performance of PbS-sensitized solar cells via controlled successive ionic-layer adsorption and reaction, PCCP, (2015).
[23] X. Zeng, W. Zhang, Y. Xie, D. Xiong, W. Chen, X. Xu, M. Wang, Y.-B. Cheng, Low-cost porous Cu2ZnSnSe4 film remarkably superior to noble Pt as counter electrode in quantum dot-sensitized solar cell system, J. Power Sources, 226 (2013) 359-362.
[24] J. Soo Kang, M.-A. Park, J.-Y. Kim, S. Ha Park, D. Young Chung, S.-H. Yu, J. Kim, J. Park, J.-W. Choi, K. Jae Lee, J. Jeong, M. Jae Ko, K.-S. Ahn, Y.-E. Sung, Reactively sputtered nickel nitride as electrocatalytic counter electrode for dye- and quantum dot-sensitized solar cells, Sci. Rep., 5 (2015) 10450.
[25] S.K. Swami, N. Chaturvedi, A. Kumar, R. Kapoor, V. Dutta, J. Frey, T. Moehl, M. Grätzel, S. Mathew, M.K. Nazeeruddin, Investigation of electrodeposited cobalt sulphide counter electrodes and their application in next-generation dye sensitized solar cells featuring organic dyes and cobalt-based redox electrolytes, J. Power Sources, 275 (2015) 80-89.
[26] U. Opara Krašovec, M. Berginc, M. Hočevar, M. Topič, Unique TiO2 paste for high efficiency dye-sensitized solar cells, Sol. Energy Mater. Sol. Cells, 93 (2009) 379-381.
[27] K. Wijeratne, J. Akilavasan, M. Thelakkat, J. Bandara, Enhancing the solar cell efficiency through pristine 1-dimentional SnO2 nanostructures: Comparison of charge transport and carrier lifetime of SnO2 particles vs. nanorods, Electrochim. Acta, 72 (2012) 192-198.
[28] J.-W. Lee, D.-Y. Son, T.K. Ahn, H.-W. Shin, I.Y. Kim, S.-J. Hwang, M.J. Ko, S. Sul, H. Han, N.-G. Park, Quantum-Dot-Sensitized Solar Cell with Unprecedentedly High Photocurrent, Sci. Rep., 3 (2013).
[29] J.G. Radich, R. Dwyer, P.V. Kamat, Cu2S Reduced Graphene Oxide Composite for High-Efficiency Quantum Dot Solar Cells. Overcoming the Redox Limitations of S2–/Sn2– at the Counter Electrode, The Journal of Physical Chemistry Letters, 2 (2011) 2453-2460.
[30] C.S. Kim, S.H. Choi, J.H. Bang, New Insight into Copper Sulfide Electrocatalysts for Quantum Dot-Sensitized Solar Cells: Composition-Dependent Electrocatalytic Activity and Stability, ACS Applied Materials & Interfaces, 6 (2014) 22078-22087.
[31] N. Al Dahoudi, Q. Zhang, G. Cao, Low-Temperature Processing of Titanium Oxide Nanoparticles Photoanodes for Dye-Sensitized Solar Cells, Journal of Renewable Energy, 2013 (2013) 8.
[32] S.-H. Chang, M.-D. Lu, Y.-L. Tung, H.-Y. Tuan, Gram-Scale Synthesis of Catalytic Co9S8 Nanocrystal Ink as a Cathode Material for Spray-Deposited, Large-Area Dye-Sensitized Solar Cells, ACS Nano, 7 (2013) 9443-9451.
[33] J.D. Roy-Mayhew, D.J. Bozym, C. Punckt, I.A. Aksay, Functionalized Graphene as a Catalytic Counter Electrode in Dye-Sensitized Solar Cells, ACS Nano, 4 (2010) 6203-6211.
[34] J.J. Montero-Rodrıguez, D. Schroeder, W. Krautschneider, R. Starbird, Equivalent circuit models for electrochemical impedance spectroscopy of PEDOT-coated electrodes.
[35] T.N. Murakami, S. Ito, Q. Wang, M.K. Nazeeruddin, T. Bessho, I. Cesar, P. Liska, R. Humphry-Baker, P. Comte, P. Péchy, Highly efficient dye-sensitized solar cells based on carbon black counter electrodes, J. Electrochem. Soc., 153 (2006) A2255-A2261.

Figure captions

Fig. 1 (a) Current-voltage measurement of Cu_2S, CoS and NiS on FTO glass substrate, (b) Current-voltage measurement of Cu_2S, CoS and NiS on brass substrate. (c)External quantum efficiency measurements of Cu_2S, CoS and NiS on FTO glasssubstrate and (d)External quantum efficiency measurements of Cu_2S, CoS and NiS on brass substrate. A, B, C are represented by Cu_2S, CoS and NiS on FTO respectively while D, E, F are represented by Cu_2S, CoS and NiS on brass respectively. G denote platinum counter electrode.

Fig. 2 Surface SEM images of (a) Cu_2S/FTO (b) Cu_2S/ brass (c) CoS/FTO (d) CoS/ brass (e) NiS/FTO (f) NiS/brass respectively.

Fig. 3A, B and C are the XRD patterns of Cu_2S, CoS and NiS on FTO glass platerespectively.

Fig. 4 (a) A, B and C are the cyclic voltammetry analysis of CEs of Cu_2S, CoS and NiS on FTO glass respectively. (b) D, E and F are the cyclic voltammetry analysis of CEs of Cu_2S, CoS and NiS on brass substraterespectively while G is the Pt CE.

Fig. 5(a) Multi-cyclic voltammetry of Cu_2S/FTO (curve A), CoS/FTO (curve B) and NiS/FTO (curve C). (b) multi-cyclic voltammetry of Cu_2S/brass (curve D), CoS/brass (curve E) and NiS/brass (curve E).

Fig. 6 Temporal variations of current density (Jsc), Voltage (Voc), fill factor (FF) and efficiency. A and D are the CEs of Cu_2S/FTO and Cu_2S/brass respectively.

Fig.7 (a) A, B and C are the EIS measurements of Cu_2S, CoS and NiS on FTO glass substrate respectively. Equivalent circuit model is shown as insert. (b) D, E and F are the EIS measurements of Cu_2S, CoS and NiS on brass substrate respectively while G denotes platinum CE. Magnified image is shown as an insert.

Fig.8 (a) A, B and C are the Tafel polarization curves of Cu_2S, CoS and NiS on FTO glass substrate respectively and (b) D, E and F are the polarization curves of Cu_2S, CoS and NiS on brass substrate respectively while G denotes platinum CE.

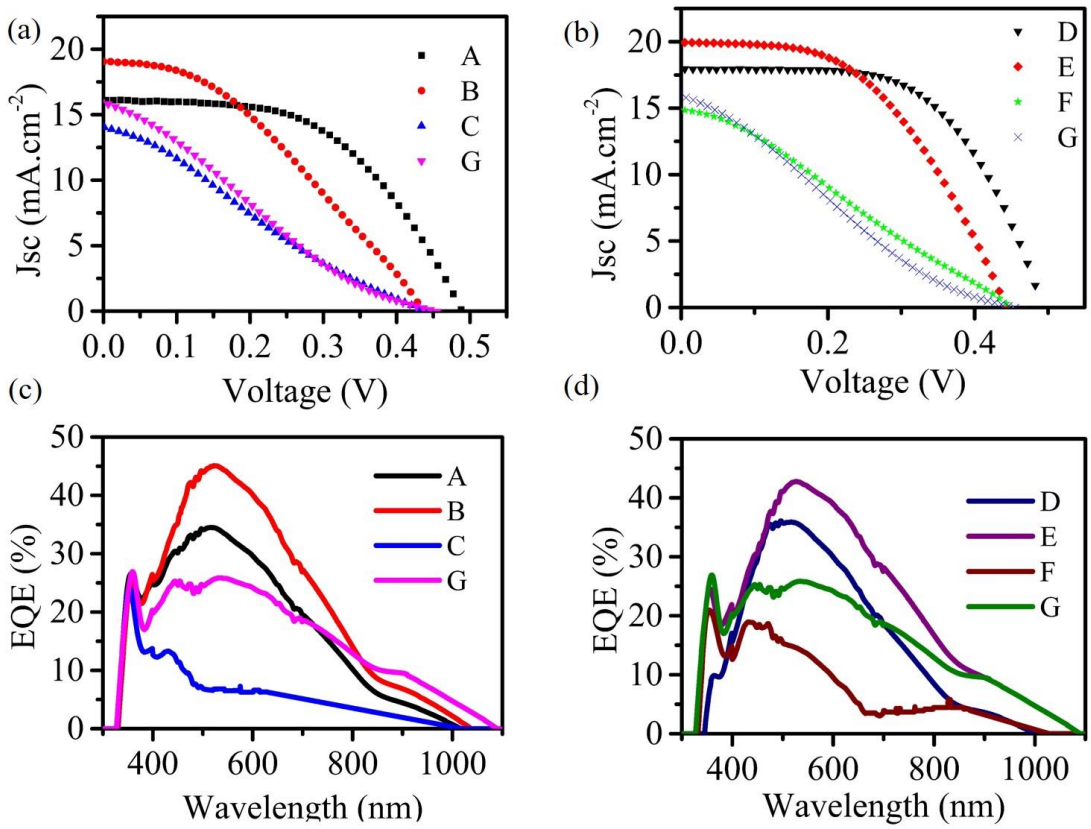

Figure 1

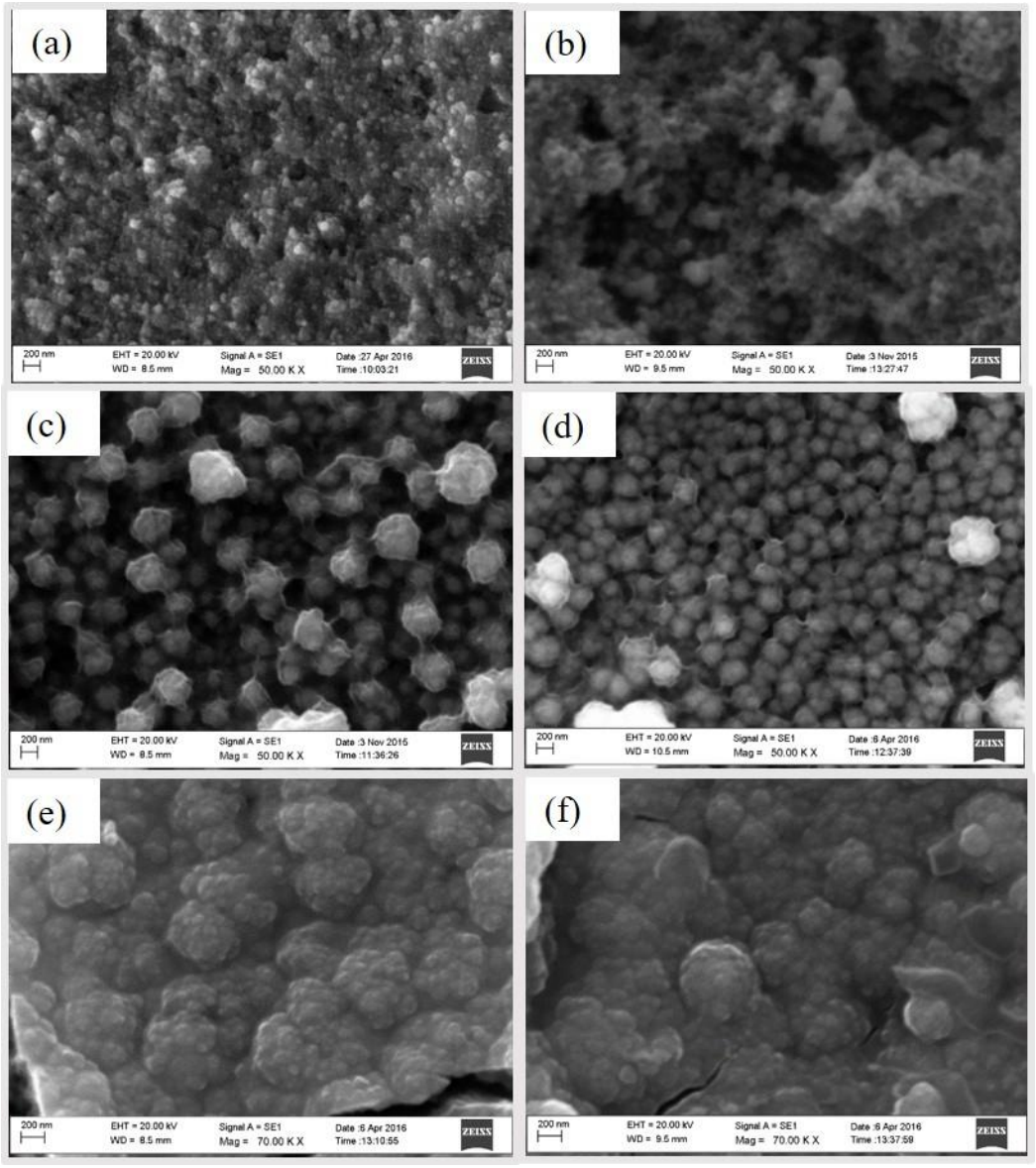

Figure 2

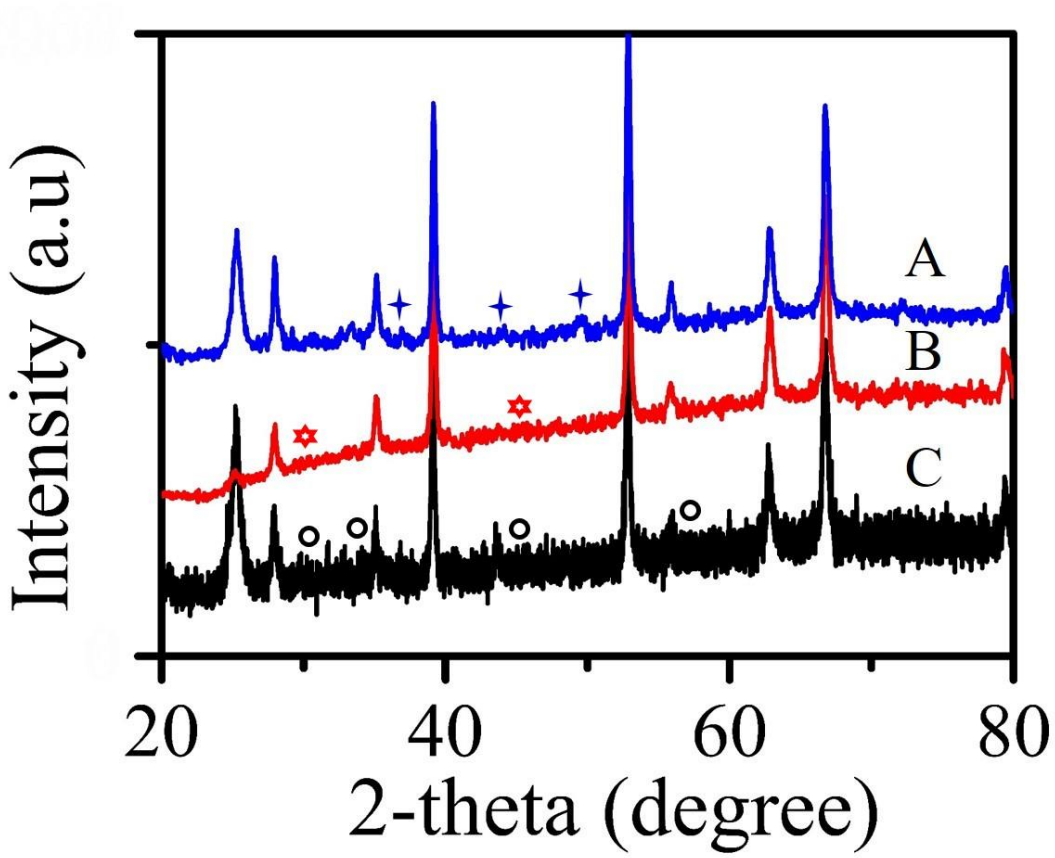

Figure 3

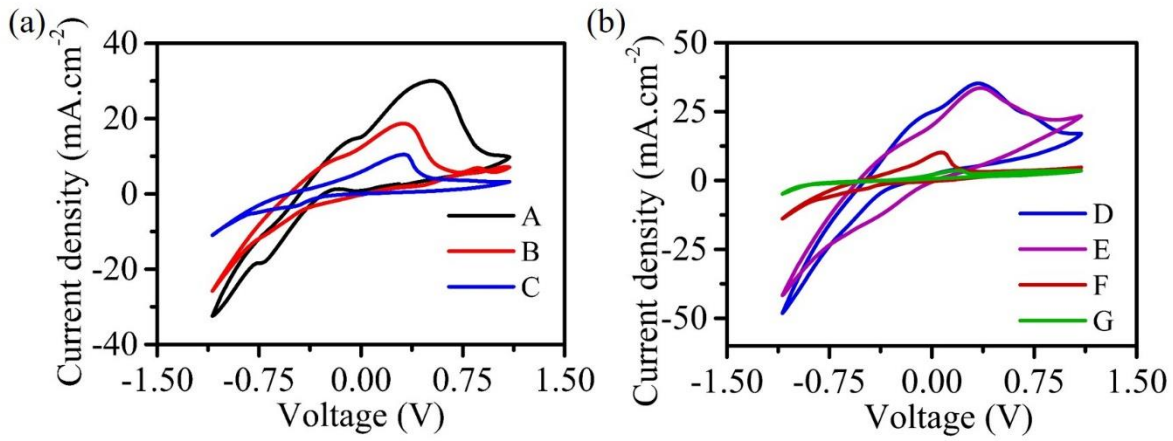

Figure 4

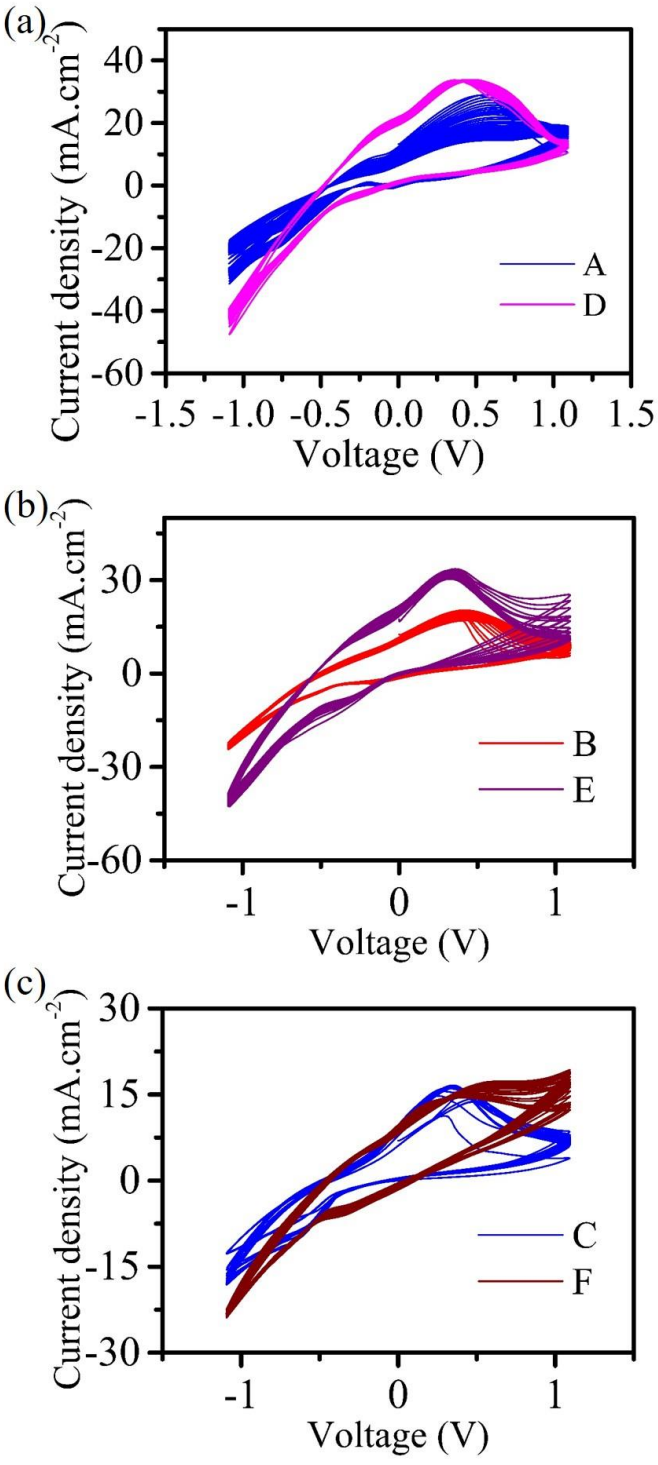

Figure 5

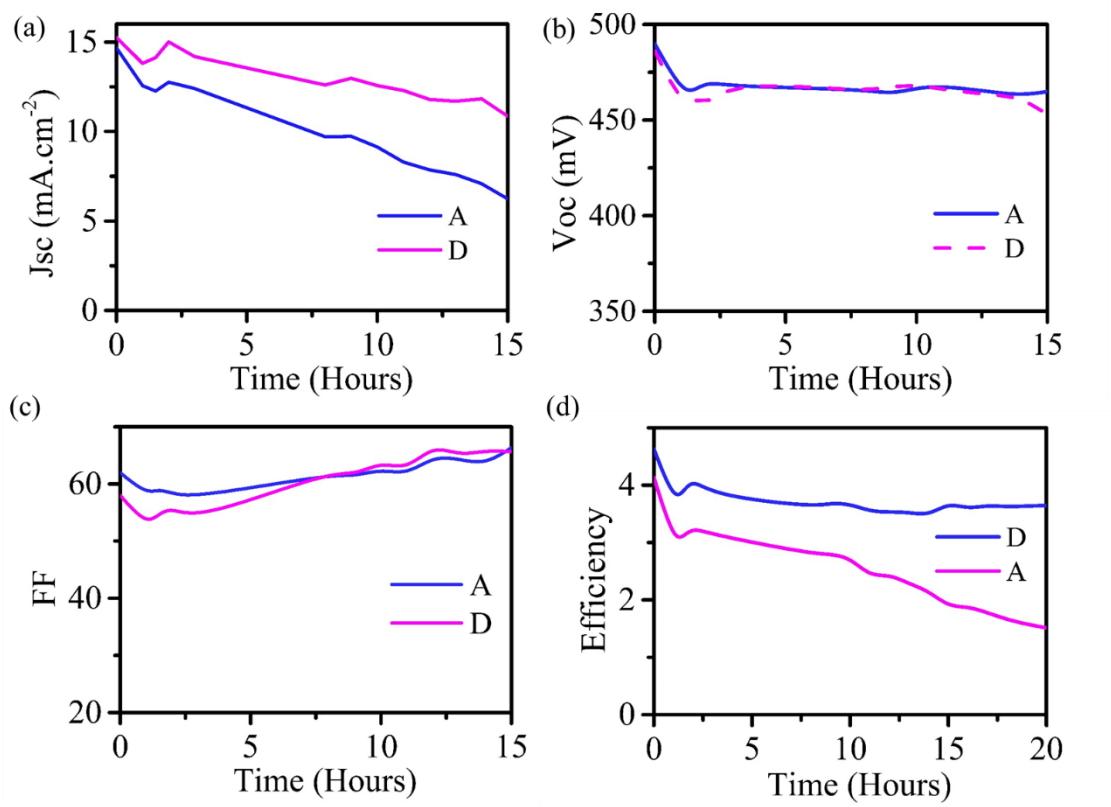

Figure 6

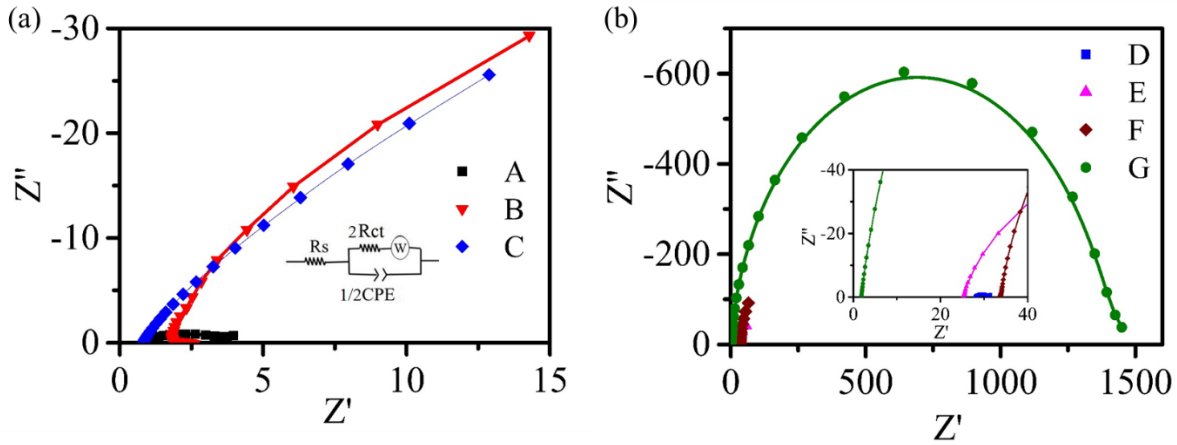

Figure 7

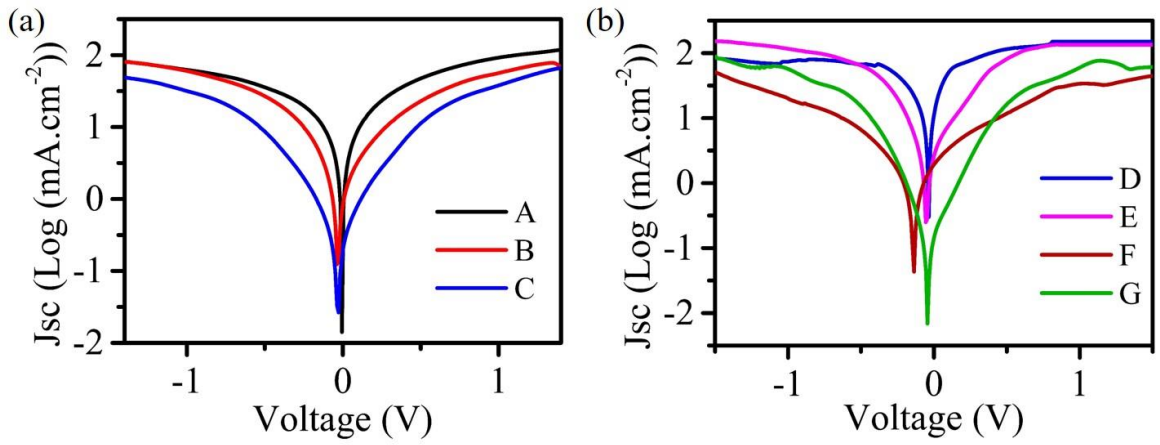

Figure 8

Table 1. Current voltage measurements of PbS/ CdS q-dots solar cells with different counter electrodes. Cu_2S, CoS and NiS on FTO glass are denotes as A, B, C while Cu_2S, CoS and NiS on brass plate denote as D, E, F respectively. G denote platinum counter electrode.

	Jsc ($mA.cm^{-2}$)	Voc (mV)	FF	Eff.
A	16.1	489.4	52.9	4.2
B	19.0	440.0	36.0	3.0
C	14.0	439.8	24.2	1.5
D	17.9	494.5	59.0	5.2
E	19.8	444.0	49.3	4.4
F	14.8	453.1	27.1	1.8
G	15.8	456.4	23.0	1.7

Table 2.Summary of cyclic voltammetry analysis of Cu_2S, CoS and NiS on FTO glass and brass plate. Cu_2S, CoS and NiS on FTO glass are denotes as A, B, C while Cu_2S, CoS and NiS on brass plate denote as D, E, F respectively. G denote platinum counter electrode. Where Ec, Ea, Epp and Ipc denotes cathodic peak potential, anodic peak potential, peak to peak splitting and cathodic peak current.

	Ec (V)	Ea (V)	Epp (V)	Ipc (mA)
A	0.525	-0.009	0.516	29.99
B	0.327	-0.156	0.483	18.67
C	0.327	-0.485	0.812	10.46
D	0.327	-0.134	0.461	35.04
E	0.240	-0.215	0.455	33.60
F	0.086	-0.485	0.571	10.11
G	0.206	-0.178	0.384	3.62

Table 3.Summary of EIS analysis and diffusion coefficient. EIS fitting errors computed using z-view software included as Chi-squared value (χ^2) and sum of square values (SS).(Diffusion coefficient derived from tafel polarization curve of Cu_2S, CoS and NiS on FTO glass and brass plate. Cu_2S, CoS and NiS on FTO glass are denotes as A, B, C while Cu_2S, CoS and NiS on brass plate denote as D, E, F respectively. G denote platinum counter electrode.

	Rs (Ω)	Rct (Ω)	CPE ($mF.cm^{-2}$)	n	χ^2	SS	D ($x10^{-6}$ cm^2s^{-1})
A	28.0	1.6	0.0534	0.66	0.00012	0.0070	1.42
B	25.2	4.8	0.0066	0.88	0.00022	0.013	1.52
C	33.7	14.5	5.3E-05	0.94	0.000024	0.0010	0.83
D	0.8	1.4	0.0602	0.69	0.0006	0.026	2.21
E	1.8	3.7	1.31E-03	1.00	0.00044	0.013	2.49
F	0.8	12.5	1.08E-04	0.90	0.0072	0.035	0.85
G	1.8	694.0	1.01E-04	0.91	0.0022	0.030	1.10